EUROPEAN FUSION DEVELOPMENT AGREEMENT

EFDA–JET–CP(03)01-74

G. Maddaluno and V. Greco

Refractive Endoscope for Wide-Angle Thermography on JET

Refractive Endoscope for Wide-Angle Thermography on JET

G. Maddaluno[1] and V. Greco[2]

[1]*ENEA-Euratom Association, Via E. Fermi 45, 00044 Frascati, Roma, Italy*
[2]*National Institute of Applied Optics – Largo E. Fermi, 6 – 50125 Firenze, Italy*

Preprint of Paper to be submitted for publication in Proceedings of the
EPS Conference on Controlled Fusion and Plasma Physics,
(St. Petersburg, Russia, 7-11 July 2003)

‘‘This document is intended for publication in the open literature. It is made available on the understanding that it may not be further circulated and extracts or references may not be published prior to publication of the original when applicable, or without the consent of the Publications Officer, EFDA, Culham Science Centre, Abingdon, Oxon, OX14 3DB, UK.”

“Enquiries about Copyright and reproduction should be addressed to the Publications Officer, EFDA, Culham Science Centre, Abingdon, Oxon, OX14 3DB, UK.”

ABSTRACT.
The capability of monitoring the entire cross section of a tokamak vacuum chamber with an infrared camera can allow both the fulfilling of discharge energy balance to be attained and the existence of impurity generating hot spots to be discovered. In this work an endoscope based on refractive optics has been designed for the wide-angle thermography to be installed on JET. The optical code CODE V [1] was used. Even if reflective optics is presently preferred for ITER relevant diagnostics, nevertheless the present design can be considered a valid back-up solution.

1. DESCRIPTION OF THE OPTICAL SYSTEM

The system allows an area as large as the JET poloidal cross-section (Fig.1) to be imaged with a depth of field of 4500mm, centred at 4250mm from the end of the endoscope.

Both infrared and visible light is transmitted through the system, the transmission band of used lens material (Multispectral grade Zinc sulphide) ranging from 0.5 to 14mm. In order to reduce chromatic aberrations and dynamic range, the width of IR wavelength band was reduced to 200nm. Following the choice taken for C-Mod [2] the band was centred around 4.3mm. Optimisation in the visible range was carried out for a wavelength band, 100nm wide, centred on the Hα emission line. The endoscope is axisymmetric and no aspherical surfaces are included in the design. The on-axis f-number and reduction factor are 3 and 3.6×10^{-3}, for the IR endoscope channel, and 3.6 and 1.8×10^{-3} for the visible one. The Numerical Aperture in Object space (NAO) is 6.0×10^{-4} (2.5×10^{-4}) and the diameter of the entrance pupil is 5.3 (2.3) mm for IR (visible) channel. The part of collecting optics shared by both IR and visible channels consists of 8 Multispectral grade Zinc sulphide (ZnS) lenses, 2 sapphire windows, 5 plane mirrors and one beam splitter, separating IR and visible channels. The first four lenses and two plane mirrors form a telecentric objective, with a reduction ratio of about 85:1 (see Fig.2). The image produced is then transported to the beam splitter by one and half relays, consisting of four equal lenses. The final IR image come in through an objective consisting of five lenses, one plane mirror, one IR filter and is focused on a Focal Plane Array (FPA) with 640×512 pixels and a 25mm pitch. The cold shield of the camera represents the stop of the endoscope IR channel. The visible image comes in through an other, separated objective and is focused on a 2/3 " CCD array (8.86.6mm, 6mm pixel size). The Field of View (FOV) is $\pm 32^{o}$ in the vertical direction, $\pm 25^{o}$ in the horizontal direction and $\pm 35^{o}$ along the diagonals. Taking into account the distortion introduced by the optical system, this corresponds to almost the full coverage of the FPA and CCD pixels by the object image. The supporting structure of refractive optics consists of 5 (6) sections for IR (visible) channel. The first one is 2253 mm long in the radial direction and is supposed to be installed in the lower limiter guide tube on octant 8. A schematic view of the supporting structure is shown in Fig. 3. The long, complex optical path is necessary because infrared camera and CCD (represented by the two boxes) need to be located behind the KJ5 concrete to avoid irradiation problems.

Because of the presence of the lenses, cooling of the first radial section of the optical system is mandatory, wall operating temperature as high as 300^{o}C being foreseen. In order to allow the allocation

of a cooling jacket, the diameter of all the five lenses in the first radial section is not larger than 92!mm. By allowing for ZnS internal transmission of about 80% (value obtained scaling available data with used thickness) and for 1% reflection by each surface, the total transmittance of the optical system results to be ~2%.

2. RADIOMETRIC CONSIDERATIONS

Despite the rather poor transmittance of the optical system, the high sensitivity of nowadays infrared camera guarantees that incident radiation is sufficient for a reliable temperature measurement. For an object plane at 4250mm from the endoscope entrance, an object temperature of 150^{o}C (the minimum temperature to be measured) and assuming a FOV of $\pm 35^{o}$ in the vertical direction and $\pm 25^{o}$ in the horizontal direction, an area as large as 22m^2 is imaged by the optical system. The power emitted by a black-body at temperature 150^{o}C, in the wavelength range between 4.2 and 4.4μm and assuming an emissivity 0.8, is $P_{4.2\text{-}4.4\,\mu m} = 15 W/m^2$. Therefore the object plane emits about 320W. By allowing for a Numerical Aperture in Object space (NAO) of 6.0×10^{-4}, a fraction $\Omega/2\pi = 1.9 \times 10^{-7}$ of this power is accepted by the optical system. This means that for uniform object temperature and allowing for an overall system transmission of 2%, the FPA receives about 1.0×10^{-6} W. In order to evaluate if this power can allow a reliable temperature measurement, it must be compared with the NEP (Noise Equivalent Power) of commercial radiometric cameras. Usually infrared camera are characterized by the normalised detectivity D*, that is related to NEP by the relation $NEP = (A_d \times \Delta f)^{1/2} / D^*$ where A_d is the detector area and Δf is the noise equivalent bandwith, normally given by $1/2\tau$ with τ = integration time. In our case, with $A_d = 2.048 cm^2$, $\tau = 1$ ms and a typical D* of 2×10^{11} cm $\sqrt{Hz}/W$, we get a NEP value of 1.6×10^{-10} W, well below the minimum power falling on the detector.

3. SPATIAL RESOLUTION

The performance of the system in terms of spatial resolution is analysed through the spot diagrams. In Fig. 4 the spot diagram for five points of the object space as imaged on the FPA is shown for the wavelength band 4.2-4.4 mm. From bottom to top the spots refer to object points at 4250 mm from the endoscope, with FOV of 0^{o}, 10^{o}, 20^{o}, 30^{o} and 35^{o}. By changing this distance within the depth of field, only minor changes in spot diameter are observed. From the figure it can be deduced that the radius of the circle containing the 84% of the focused energy is of the order of the pitch of the FPA. Then, by using ray tracing techniques in calculating the reduction factor and according to the Rayleigh criterion [3], in the infrared range, for a distance object-endoscope of 2000, 4250 and 6500 mm, the endoscope/ camera system allows two point sources separated by 3.3, 6.8, 10.4mm, on axis, and 4.7, 9.8, 15mm, at full field respectively, to be spatially resolved. Allowing a 30 mm displacement of the JET vessel with respect to the outside optics does not degrade the spatial resolution. This results from an image of cold stop falling in the proximity of the second sapphire window. From the fact that the radius of spots on the image plane could not be reduced beyond the FPA pitch, because of chromatic aberration introduced by the 13 lenses, we deduce that zooming in the infrared range is probably ineffective.

CONCLUSIONS

A refractive IR-visible endoscope has been designed for the wide-angle thermography to be installed on JET. Geometrical constrains as well as the long optical path required for locating infrared and visible camera behind the KJ5 concrete result in a rather poor transmittance of the system. Nevertheless the high sensitivity of present commercial infrared camera allows reliable temperature measurements. The good performance in terms of field of view, spatial resolution and depth of field make this refractive endoscope a valid back-up alternative to the more ITER relevant solution based on reflective optics.

ACKNOWLEDGEMENTS

Work carried out under contract EFDA 02/680

REFERENCES

[1]. Optical Research Associates, 3280 East Foothill Boulevard, Suite 300 Pasadena, California 91107 USA.

[2]. R. J. Maqueda et al., Rev. Sci. Instrum. **70**, 734 (1999) .

[3]. M. Born, E. Wolf, "Principles of optics", Cambridge University Press, pp. **439-44**3, (1999)

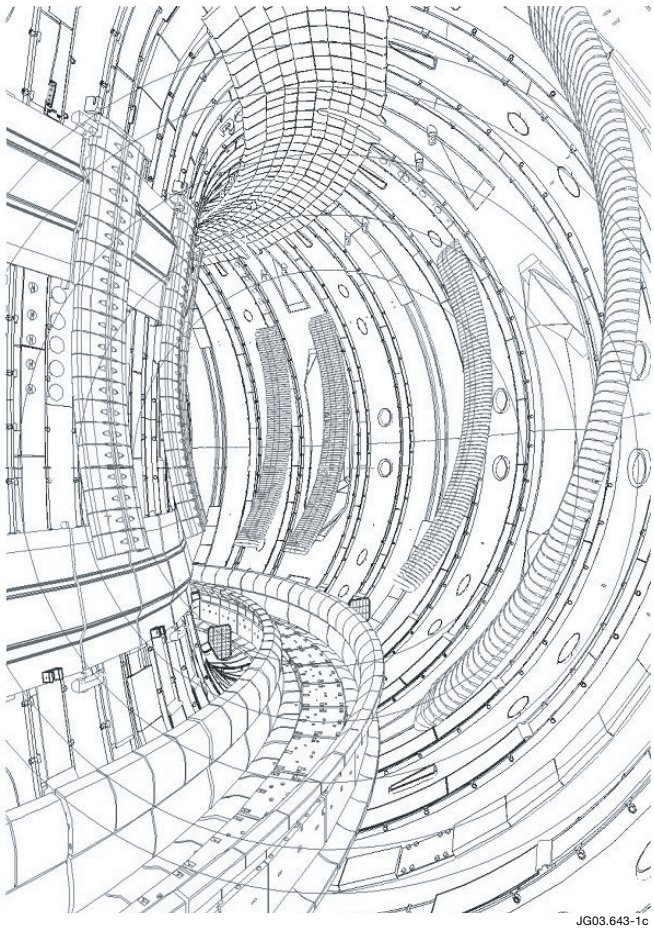

Figure 1: View through endoscope in JET with a 20°, 25°, 30°, 35° and 38° FOV

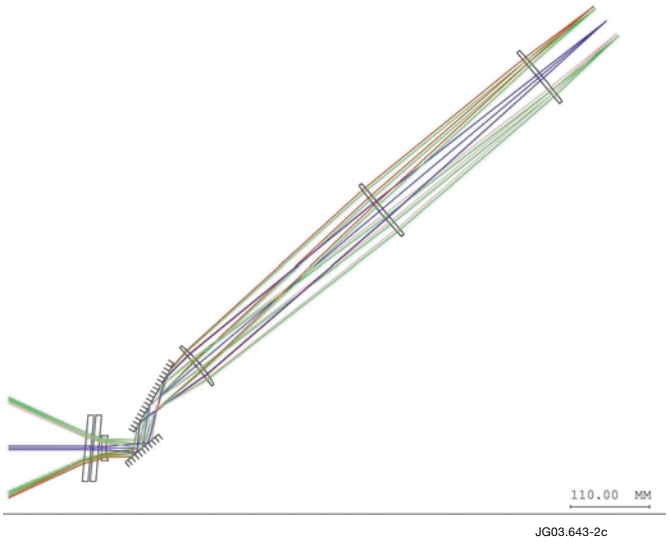

Figure 2: Telecentric objective. The ray tracing is reported for different object points at l = 4.3mm.

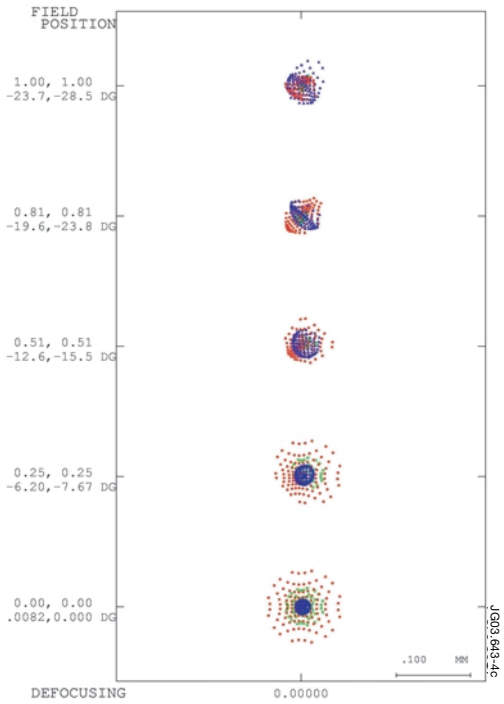

Figure 4: Spot diagram relative to points with 0^o, 10^o, 20^o, 30^o and 35^o FOV.

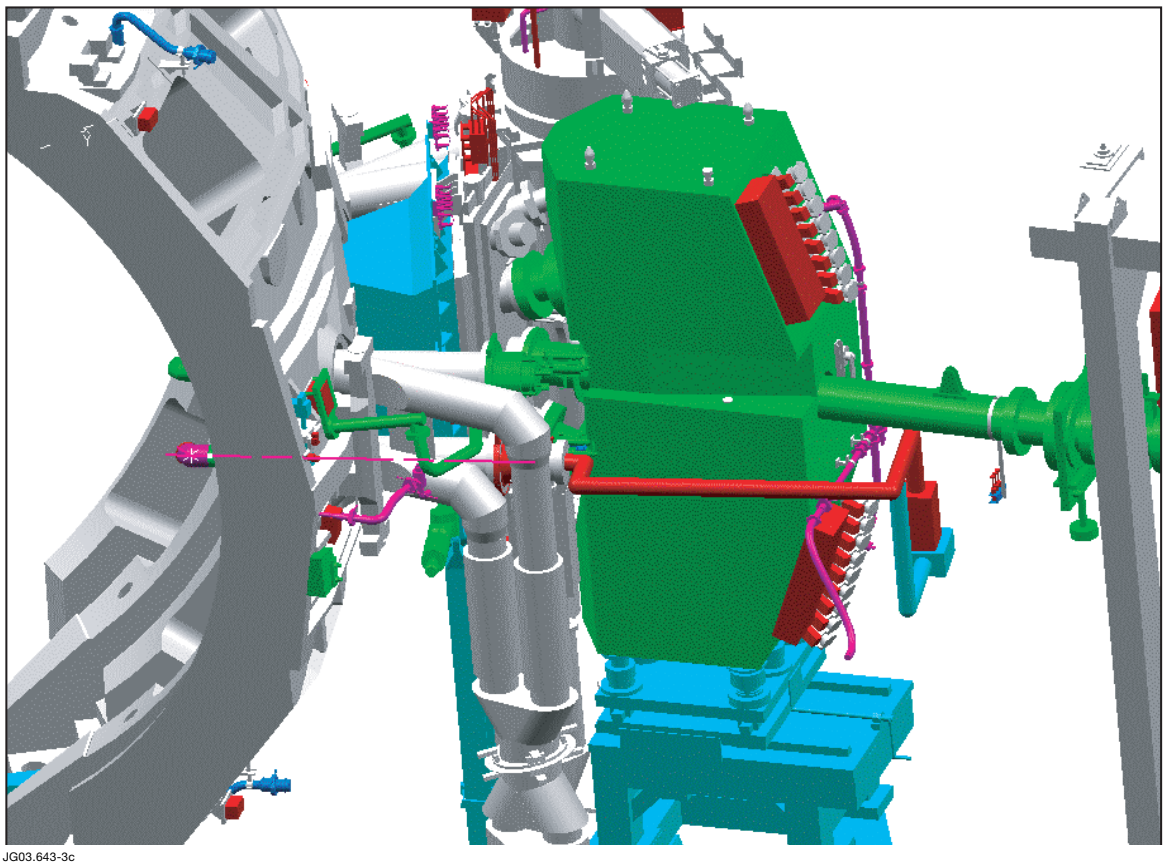

Figure 3: Schematic view of the structure (red/cyan tube) supporting endoscope optics.